Coherent state model extension for the description of positive and negative parity bands in even-odd nuclei

A. A. Raduta,[1,2,3] C. M. Raduta,[2] and Amand Faessler[4]

[1]*Department of Theoretical Physics and Mathematics, Bucharest University, Post Office Box MG11, Bucharest RO-077125, Romania*
[2]*Department of Theoretical Physics, Institute of Physics and Nuclear Engineering, Post Office Box MG6, Bucharest RO-077125, Romania*
[3]*Academy of Romanian Scientists, 54 Splaiul Independentei, Bucharest RO-050094, Romania*
[4]*Institut für Theoretische Physik der Universität Tübingen, Auf der Morgenstelle 14, D-72076 Tübingen, Germany*

A particle-core Hamiltonian is used to describe the lowest parity partner bands, $K^\pi = 1/2^\pm$, in ^{219}Ra, ^{237}U, and ^{239}Pu and three pairs of parity partner bands, $K^\pi = 1/2^\pm$, $3/2^\pm$, and $5/2^\pm$, in ^{227}Ra. The core is described by a quadrupole and octupole boson Hamiltonian. The particle-core Hamiltonian consists of four terms: a quadrupole-quadrupole, an octupole-octupole, a spin-spin, and a rotational $\hat{I}^2$ interaction, with $\hat{I}$ denoting the total angular momentum. The model Hamiltonian is treated within a projected spherical particle-core basis. The calculated excitation energies are compared with the corresponding experimental data as well as with those obtained using other approaches. For ^{219}Ra, we also calculated the $E1$ and $E2$ branching ratios. Also, we searched for some signatures for static octupole deformation in the considered odd isotopes.

I. INTRODUCTION

Formalisms devoted to the description of the experimental spectra [1–4] of even-odd nuclei are based on particle-core interaction [5–13]. Thus, properties of the even-even core and the odd particle contribute coherently to the energy levels of the odd system. Depending on the nature of the particle-core interaction, whether it is a weak or strong coupling regime, the odd system is treated in either the laboratory or an intrinsic reference frame. Working in the intrinsic reference frame is advantageous because the function dependent on the Euler angles is fully separated, and consequently the angular momentum projection on the z axis of the intrinsic frame, K, becomes a good quantum number. Thus in Refs. [10–13], spectra of some odd isotopes were studied by using a quadrupole-octupole Hamiltonian in the intrinsic deformation variables β_2 and β_3 separated in a kinetic energy term, a potential energy term, and a Coriolis interaction. Because of the specific structure of the model Hamiltonian, an analytical solution for the excitation energies in the two bands of opposite parities was possible. It was shown that the split of the parity partner bands was determined by a combined effect coming from the Coriolis interaction, which affects the $K = 1/2$ bands, and a quantum number k associated with the motion of a phase angle ϕ, characterizing both the quadrupole and the octupole deformation variables. Based on analytical calculations, some conclusions concerning the $B(E2)$ values associated with the intraband transitions between states of similar parities were drawn. Thus, if the odd particle state is of positive parity, the transitions between positive parity states are enhanced, in contrast to those connecting negative parity states. If the parity of the odd particle state is negative, the ordering of those transitions is reversed. In Ref. [9], the equilibrium deformations were calculated independently for each quasiparticle, and moreover the states were not of definite parity. However, they were characterized by the same K if they belong to the same band.

The core system is usually described by the Bohr-Mottelson liquid-drop model or by a rotor model. Of course, such models are unable to account for the complex structure of the core. However, for the sake of simplicity, the terms associated with the core are adopted for describing the odd-system properties. Thus, one implicitly assumes that only part of the core properties is influencing the odd-particle motion. In this context, it would be desirable to have a consistent description of the even-even and even-odd nuclei. In the present article, we attempt to present a possible approach with this feature.

The coherent state model (CSM) [14] describes in a realistic fashion three interacting bands (ground, β, and γ) in terms of quadrupole bosons. The formalism was later extended [15–20] by considering the octupole degrees of freedom. The most recent extension described eight rotational bands, four of positive parity and four of negative parity. Observables such as excitation energies, intraband $E2$ reduced transition probabilities, and interband $E1$, $E2$, and $E3$ reduced transition probabilities were calculated, and the results were compared with the corresponding experimental data. The formalism works well for both near-spherical and deformed nuclei excited in low and high angular momentum states. Indeed, we considered all states with $J \leqslant 30$ in both the positive and the negative parity bands. Signatures for a static octupole deformation in ground as well as in excited bands have been pointed out in several even-even nuclei.

The aim of this article is to extend the CSM for the even-odd nuclei that exhibit both quadrupole and octupole deformation.

The formalism concerning the excitation energies in the positive and negative parity bands is presented in Secs. II and III. The $E1$ and $E2$ transitions are considered in Sec. IV, and the numerical application to four even-odd nuclei is described in Sec. V. Final conclusions are drawn in Sec. VI.

II. THE MODEL HAMILTONIAN

We suppose that the rotational bands in even-odd nuclei may be described by a particle-core Hamiltonian,

$$H = H_{sp} + H_{core} + H_{pc}, \quad (2.1)$$

where H_{sp} is a spherical shell model Hamiltonian associated with the odd nucleon and H_{core} is a phenomenological Hamiltonian that describes the collective motion of the core in terms of quadrupole and octupole bosons. This term is identical to that used in Ref. [20] to describe eight rotational bands in even-even nuclei. The two subsystems interact with each other by H_{pc}, which has the following expression:

$$H_{pc} = -X_2 \sum_{\mu} r^2 Y_{2,-\mu}(-)^{\mu}(b_{2\mu}^{\dagger} + (-)^{\mu} b_{2,-\mu})$$
$$- X_3 \sum_{\mu} r^3 Y_{3,-\mu}(-)^{\mu}(b_{3\mu}^{\dagger} + (-)^{\mu} b_{3,-\mu})$$
$$+ X_{jJ} \vec{j} \cdot \vec{J} + X_{I^2} \vec{I}^2. \quad (2.2)$$

The term $b_{\lambda\mu}^{\dagger}$ denotes the components of the λ-pole (with $\lambda = 2, 3$) boson operator. The term $\vec{j} \cdot \vec{J}$ is similar to the spin-orbit interaction from the shell model and expresses the interaction between the angular momenta of the odd particle and the core. Treated in the intrinsic reference frame, this term expresses the Coriolis interaction up to a particle-particle recoil energy term $j \cdot j$. The last term is due to the rotational motion of the whole system, and $\vec{I}$ denotes the total angular momentum of the particle-core system.

The core states are described by eight sets of mutually orthogonal functions obtained by projecting the angular momentum and the parity from four quadrupole and octupole deformed functions. One is a product of two coherent states,

$$\Psi_g = e^{f(b_{30}^{+} - b_{30})} e^{d(b_{20}^{+} - b_{20})} |0\rangle_2 |0\rangle_3 \equiv \Psi_o \Psi_q |0\rangle_2 |0\rangle_3, \quad (2.3)$$

and the remaining three are polynomial boson excitations of Ψ_g. The parameters d and f are real numbers and simulate the quadrupole and octupole deformations, respectively. The vacuum state for the λ-pole boson, $\lambda = 2, 3$, is denoted by $|0\rangle_{\lambda}$.

The particle-core interaction generates a deformation for the single-particle trajectories. By averaging the model Hamiltonian with Ψ_g, one obtains a deformed single-particle Hamiltonian, H_{mf}, which plays the role of the mean field for the particle motion:

$$H_{mf} = \mathcal{C} + H_{sp} - 2dX_2 r^2 Y_{20} - 2f X_3 r^3 Y_{30}, \quad (2.4)$$

where $\mathcal{C}$ is a constant determined by the average of H_{core}. The Hamiltonian H_{mf} represents an extension of the Nilsson Hamiltonian by adding the octupole deformation term. In Ref. [21], we have shown that to get the right deformation dependence of the single-particle energies H_{mf} must be amended with a monopole-monopole interaction, $M\omega^2 r^2 \alpha_{00} Y_{00}$, where the monopole coordinate α_{00} is determined from the volume conservation restriction. This term has a constant contribution within a band. However, the constant value is band dependent.

To find the eigenvalues of the model Hamiltonian, we follow several steps:

(i) In principle, the single-particle basis could be determined by diagonalizing H_{mf} amended with the monopole interaction. The product basis for particle and core may be used further to find the eigenvalues of H. Because of some technical difficulties in restoring the rotation and space-reversal symmetries for the composite system wave function, this procedure is tedious, and therefore we prefer a simpler method. Thus, the single-particle space consists of three spherical shell model states with angular momenta j_1, j_2, and j_3. We suppose that j_1 and j_2 have the parity $\pi = +$ and that j_3 has the parity $\pi = -$.

(ii) Ψ_g is a sum of two states of different parities. This happens because of the specific structure of the octupole coherent state:

$$\Psi_o = \Psi_o^{(+)} + \Psi_o^{(-)}. \quad (2.5)$$

The states of a given angular momentum and positive parity can be obtained through projection from the intrinsic states

$$|n_1 l_1 j_1 K\rangle \Psi_o^{(+)} \Psi_q, \quad |n_2 l_2 j_2 K\rangle \Psi_o^{(+)} \Psi_q,$$
$$|n_3 l_3 j_3 K\rangle \Psi_o^{(-)} \Psi_q. \quad (2.6)$$

The projected states of negative parity are obtained from the states

$$|n_1 l_1 j_1 K\rangle \Psi_o^{(-)} \Psi_q, \quad |n_2 l_2 j_2 K\rangle \Psi_o^{(-)} \Psi_q,$$
$$|n_3 l_3 j_3 K\rangle \Psi_o^{(+)} \Psi_q. \quad (2.7)$$

The angular momentum and parity projected states are denoted by

$$\varphi_{IM}^{(+)}(j_i K; d, f) = N_{i;IK}^{(+)} P_{MK}^{I} |n_i l_i j_i K\rangle \Psi_o^{(+)} \Psi_q$$
$$\equiv N_{i;IK}^{(+)} \psi_{IM}^{(+)}(j_i K; d, f), \quad i = 1, 2,$$
$$\varphi_{IM}^{(+)}(j_3 K; d, f) = N_{3;IK}^{(+)} P_{MK}^{I} |n_3 l_3 j_3 K\rangle \Psi_o^{(-)} \Psi_q$$
$$\equiv N_{3;IK}^{(+)} \psi_{IM}^{(+)}(j_3 K; d, f),$$
$$\varphi_{IM}^{(-)}(j_i K; d, f) = N_{i;IK}^{(-)} P_{MK}^{I} |n_i l_i j_i K\rangle \Psi_o^{(-)} \Psi_q$$
$$\equiv N_{i;IK}^{(-)} \psi_{IM}^{(-)}(j_i K; d, f), \quad i = 1, 2,$$
$$\varphi_{IM}^{(-)}(j_3 K; d, f) = N_{3;IK}^{(-)} P_{MK}^{I} |n_3 l_3 j_3 K\rangle \Psi_o^{(+)} \Psi_q$$
$$\equiv N_{3;IK}^{(-)} \psi_{IM}^{(-)}(j_3 K; d, f). \quad (2.8)$$

The factors $N_{i,IK}^{(\pm)}$ ensure that the projected states $\varphi^{(\pm)}$ are normalized to unity. Obviously, the unnormalized projected states are denoted by $\psi^{(\pm)}$. For the quantum number K, we consider the lowest three values (i.e., $K = 1/2, 3/2$, and $5/2$). Note that the earlier particle-core approaches [5,6] restrict the single-particle space to a single j, which eliminates the contribution of the octupole-octupole interaction.

(iii) Note that for a given j_i, the projected states with different K are not orthogonal. Indeed, the overlap matrices

$$A_{K,K'}^{(+)}(I j_l; d, f) = \langle \psi_{IM}^{(+)}(j_l K; d, f) | \psi_{IM}^{(+)}(j_l K'; d, f)\rangle,$$
$$l = 1, 2, 3, \quad K, K' = 1/2, 3/2, 5/2;$$

$$A_{K,K'}^{(-)}(Ij_l; d, f) = \langle \psi_{IM}^{(-)}(j_lK; d, f) | \psi_{IM}^{(-)}(j_lK'; d, f) \rangle,$$
$$l = 1, 2, 3, \quad K, K' = 1/2, 3/2, 5/2, \quad (2.9)$$

are not diagonal. By diagonalization, one obtains the eigenvalues $a_{Ip}^{(\pm)}(j_l)$ and the corresponding eigenvectors $V_{IK}^{(\pm)}(j_l, p)$, with $K = 1/2, 3/2$, and $5/2$ and $p = 1, 2$, and 3. Then, the functions

$$\Psi_{IM}^{(+)}(j_l, p; d, f) = N_{l;Ip}^{(+)} \sum_K V_{IK}^{(+)}(j_l, p)$$
$$\times \psi_{IM}^{(+)}(j_lK; d, f),$$
$$\Psi_{IM}^{(-)}(j_l, p; d, f) = N_{l;Ip}^{(-)} \sum_K V_{IK}^{(-)}(j_l, p)$$
$$\times \psi_{IM}^{(-)}(j_lK; d, f) \quad (2.10)$$

are mutually orthogonal. The norms are given by

$$(N_{l;Ip}^{(\pm)})^{-1} = \sqrt{a_{Ip}^{(\pm)}(j_l)}. \quad (2.11)$$

For each of the new states, there is a term in the defining sum, Eq. (2.10), which has a maximal weight. The corresponding quantum number K is conventionally assigned to the mixed state.

(iv) To simulate the core deformation effect on the single-particle motion, in some cases the projected states corresponding to different j must be mixed up:

$$\Phi_{IM}^{(+)}(p; d, f) = \sum_{l=1,2,3} \mathcal{A}_{pl}^{(+)} \Psi_{IM}^{(+)}(j_l p; d, f),$$
$$\Phi_{IM}^{(-)}(p; d, f) = \sum_{l=1,2,3} \mathcal{A}_{pl}^{(-)} \Psi_{IM}^{(-)}(j_l p; d, f). \quad (2.12)$$

The amplitudes $\mathcal{A}_{pl}^{(\pm)}$ can be obtained either by diagonalizing H_{mf} or, as we mentioned before, by a least-squares fitting procedure applied to the excitation energies. Here, the coefficients $\mathcal{A}$ are determined by a fitting procedure. The energies of the odd system are approximated by the average values of the model Hamiltonian corresponding to the projected states:

$$E_I^{(+)}(p; d, f) = \langle \Phi_{IM}^{(+)}(p; d, f) | H | \Phi_{IM}^{(+)}(p; d, f) \rangle,$$
$$E_I^{(-)}(p; d, f) = \langle \Phi_{IM}^{(-)}(p; d, f) | H | \Phi_{IM}^{(-)}(p; d, f) \rangle. \quad (2.13)$$

The matrix elements involved in these equations can be analytically calculated. Note that because of the structure of the particle-core projected states, the energies for the odd system are determined by the coupling of the odd particle to the excited states of the core ground band.

The approach presented in this section was applied to the description of the $K^\pi = 1/2^\pm$ bands. However, this procedure can be extended by including the $K \neq 0$ states in the space describing the deformed core.

III. DESCRIPTION OF THE $K^\pi = 3/2^\pm$ AND $5/2^\pm$ BANDS

In principle, the method presented in the previous section may work for the description of bands with quantum number K greater than $1/2$. However, the intrinsic reference frame for the odd system is determined by the deformed core, and therefore one expects that this brings an important contribution to the quantum number K. To be more specific, we cannot expect to obtain a realistic description of the $K = 5/2$ bands by projecting the good angular momentum from $|j, 5/2\rangle \otimes \Psi_g$. Therefore, we assume that the $K^\pi = 3/2^\pm$ and $5/2^\pm$ bands are described by projecting the angular momentum from a product state of a low-K single-particle state and the intrinsic γ band state.

We recall that within CSM, the states of the γ band are obtained by projection from the intrinsic state

$$\Psi_2^{(\gamma;\pm)} = \Omega_{\gamma,2}^\dagger \Psi_o^{(\pm)} \Psi_q, \quad (3.1)$$

where the excitation operator for the γ intrinsic state is defined as

$$\Omega_{\gamma,2}^\dagger = (b_2^\dagger b_2^\dagger)_{22} + d\sqrt{\frac{2}{7}} b_{22}^\dagger. \quad (3.2)$$

Here, $b_{2\mu}^\dagger$ denotes the m component of the quadrupole boson operator. The low index of Ψ in Eq. (3.1) is the K quantum number for the γ intrinsic state. Thus, a simultaneous description of the bands with $K = 1/2, 3/2$, and $5/2$ can be achieved with the projected states:

$$\varphi_{IM;1/2}^{(\pm)} = N_{I,1/2}^{(\pm)} \sum_J (N_J^{(g,\pm)})^{-1}$$
$$\times C_{1/2\,0\,1/2}^{j_1\,J\,I} (|n_1l_1j_1\rangle \otimes \varphi_J^{(g;\pm)})_{IM},$$
$$\varphi_{IM;3/2}^{(\pm)} = N_{I,3/2}^{(\pm)} \sum_J (N_J^{(\gamma,\pm)})^{-1}$$
$$\times C_{-1/2\,2\,3/2}^{j_2\,J\,I} (|n_2l_2j_2\rangle \otimes \varphi_J^{(\gamma;\pm)})_{IM}, \quad (3.3)$$
$$\varphi_{IM;5/2}^{(\pm)} = N_{I,5/2}^{(\pm)} \sum_J (N_J^{(\gamma,\pm)})^{-1}$$
$$\times C_{1/2\,2\,5/2}^{j_3\,J\,I} (|n_3l_3j_3\rangle \otimes \varphi_J^{(\gamma;\mp)})_{IM}.$$

In these expressions, the notation $N_J^{(i,\pm)}$ with $i = g, \gamma$ is used for the normalization factors of the projected states describing the ground and the γ bands, respectively, of the even-even core:

$$\varphi_{JM}^{(g,\pm)} = N_J^{(g,\pm)} P_{M0}^J \Psi_g,$$
$$\varphi_{JM}^{(\gamma,\pm)} = N_J^{(\gamma,\pm)} P_{M2}^J \Psi_2^{(\gamma,\pm)}. \quad (3.4)$$

Note that for each angular momentum I, the set of three projected states is orthogonal.

The energies for the six bands with $K^\pi = 1/2^\pm, 3/2^\pm$, and $5/2^\pm$ are obtained by averaging the model Hamiltonian (2.1) with the projected states defined previously:

$$E_{I,K} = \langle \varphi_{IM;K}^{(\pm)} | H | \varphi_{IM;K}^{(\pm)} \rangle, \quad K = 1/2, 3/2, 5/2. \quad (3.5)$$

The matrix elements of the particle-core interaction are given in Appendix A.

IV. TRANSITION PROBABILITIES

For some $K = 1/2$ bands, results for the reduced $E1$ and $E2$ transition probabilities are available. They are given in terms of the branching ratios:

$$R_{I^\pi} = \frac{B(E1; I^\pi \to (I-1)^{\pi'})}{B(E2; I^\pi \to (I-2)^{\pi})}, \quad \pi' \neq \pi. \quad (4.1)$$

To describe these data, we use the wave functions defined in Sec. II. We recall that the positive parity states are obtained by coupling the spherical shell model state j_1 or j_2 to a positive parity core with a small admixture of a state coupling j_3 and a negative parity core. However, the negative parity states are given by coupling one of the states j_1 or j_2 to a negative parity core and a small component consisting of a product state of j_3 and a positive parity core state. Thus, the single-particle $E1$ transition operator may connect the leading term of the initial state with the small component of the final state. One expects that the contribution of this term to the $E1$ transition is negligible compared with the contribution of collective dipole operator. Therefore, the dipole transition operator considered in the present article is the boson operator:

$$Q_{1\mu} = eq_1[(b_2^\dagger b_3^\dagger)_{1\mu} + (b_3 b_2)_{\widetilde{1\mu}}]. \quad (4.2)$$

The quadrupole transition operator has the structure

$$Q_{2\mu} = eq_2(b_{2\mu}^\dagger + (-)^\mu b_{2,-\mu} + ar^2 Y_{2\mu}). \quad (4.3)$$

The branching ratio, Eq. (4.1), for the initial state I^π is

$$R_{I^\pi} = \left[\frac{\langle I^\pi || Q_1 || (I-1)^{\pi'} \rangle}{\langle I^\pi || Q_2 || (I-2)^{\pi} \rangle} \right]^2. \quad (4.4)$$

Here, the initial and final states are a mixture of different K states as well as a mixture of the j states defined by Eq. (2.12). The matrix elements of the transition operators between the basis states are given in Appendix B.[1]

V. NUMERICAL RESULTS

The results obtained in Sec. II have been used to calculate the excitation energies for one positive and one negative parity band in three even-odd isotopes: ^{219}Ra, ^{237}U, and ^{239}Pu. The parameters defining H_{core}, as well as the deformation parameters d and f, are those used to describe the properties of eight rotational bands in the even-even neighboring isotopes. The single-particle states are spherical shell model states with the appropriate parameters for the (N, Z) region of the considered isotopes [23]. Our calculations for the mentioned odd isotopes correspond to the single-particle states: $(j_1, j_2, j_3) = (2g_{7/2}, 2g_{9/2}, 1h_{9/2})$. To obtain the best agreement between the calculated excitation energies and the corresponding experimental data, in the expansion (2.12), a small admixture of the states $(j_1; j_3)$ and $(j_2; j_3)$ was considered: $|\mathcal{A}_{i,3}^{(+)}|^2$ and $|\mathcal{A}_{i,3}^{(-)}|^2$ are both equal to 0.001 for ^{219}Ra, whereas the amplitudes

---

[1]Throughout this article, the reduced matrix elements are defined according to Rose's convention [22].

TABLE I. Parameters involved in the particle-core Hamiltonian obtained by fitting four excitation energies. Here b denotes the oscillator length: $b = (\frac{\hbar}{M\omega})^{1/2}$; $\hbar\omega = 41A^{-1/3}$. The usual notations for nucleon mass (M) and atomic number (A) were used.

Parameters	^{219}Ra	^{227}Ra	^{237}U	^{239}Pu
$X_2 b^2$ (keV)	22.829	−1.992	1.080	−2.515
$X_3 b^3$ (keV)	−8.680	169.511	2.227	4.937
X_{jJ} (keV)	−0.292	8.553	−5.817	−3.985
X_{I^2} (keV)	4.105	4.390	4.634	5.050

take the common value $|A_{i,3}^{(+)}|^2 = |A_{i,3}^{(-)}|^2 = 0.04$ for ^{237}U and ^{239}Pu. The mixing amplitude of the states (j_1, j_2) is negligible. Energies given in Eq. (2.13) depend on the interaction strengths X_2, X_3, X_{jJ}, and X_{I^2}. These were determined by fitting four particular energies in the two bands of different parities (i.e., $K^\pi = 1/2^\pm$). The results of the fitting procedure are given in Table I. When these are inserted in Eqs. (2.13), the energies in the two bands with $K = 1/2$ are readily obtained:

$$E(I^\pm) = E_I^{(\pm)}(1; d, f) - E_{\frac{1}{2}}^{(+)}(1; d, f). \quad (5.1)$$

The theoretical results for excitation energies, listed in Table II, agree quite well with the corresponding experimental data. The levels for the three isotopes have been populated by different experiments. Indeed, the $K^\pi = 1/2^\pm$ bands have been identified in ^{219}Ra with the reaction ^{208}Pb(^{14}C,3n)^{219}Ra [2], in ^{237}U via a pickup reaction on a ^{238}U target, and in ^{239}Pu with the so-called unsafe Coulomb excitation technique [1]. Our results suggest that the dominant j component is $g_{9/2}$. Also, the dominant K component is $K = 1/2$, which in fact confirms the previous assignments. To measure for the agreement quality, we calculated the rms values for the deviations of the calculated values from the experimental ones. The results for ^{219}Ra, ^{237}U, and ^{239}Pu are 67.1, 48.97, and 31.8 keV, respectively. The agreement obtained in our approach for ^{239}Pu is better than that shown in Ref. [13]. However, the results from Ref. [13] for ^{237}U agree better with the corresponding data than do our results. Indeed, the rms values for the deviations of theoretical results from experimental data, reported in Ref. [13], are 30 and 60 keV for ^{237}U and ^{239}Pu, which should be compared with 48.97 and 31.8 keV obtained using our approach.

In calculating the rms value for ^{219}Ra, we ignored the data for the states $53/2^\pm$ because the spin assignment is uncertain. It is interesting to mention that the spectrum of ^{219}Ra has been measured by two groups [2,3] using the same reaction: ^{208}Pb(^{14}C,3n)^{219}Ra. However, for the ground state (g.s.) they assigned different angular momenta, $9/2^+$ [2] and $7/2^+$ [3]. In our approach, both assignments yield a good description of the data. However, we used $9/2^+$ because the corresponding results agree better with the experimental data than those obtained with the other option. In the quoted references, the states $[(9/2) + 2k]^+$ with $k = 0, 1, 2, \ldots$ and $[(15/2) + 2m]^-$ with $m = 0, 1, 2, \ldots$ are considered to be $K = 1/2$ states. However, some additional states are available, organized into two aside states (I and II) [3]. As shown in Table II, these states stay close in energy to the calculated $K = 1/2$ states

TABLE II. Excitation energies (keV) in ^{219}Ra, ^{237}U, and ^{239}Pu for the bands characterized by $K^\pi = 1/2^+$ and $K^\pi = 1/2^-$, respectively. The results of our calculations (Th.) for ^{237}U and ^{239}Pu are compared with the corresponding experimental data (Exp.) taken from Ref. [1]. Experimental data (Exp.) for ^{219}Ra were taken from Ref. [2] for $I^+ = (9/2 + 2k)^+$, $k = 0, 1, 2, \ldots$ and $I^- = (13/2 + 2m)^-$, $m = 0, 1, 2, \ldots$. Experimental data for the remaining states were taken from Ref. [3].

J	^{219}Ra				^{237}U				^{239}Pu			
	$\pi = +$		$\pi = -$		$\pi = +$		$\pi = -$		$\pi = +$		$\pi = -$	
	Exp.	Th.	Exp.	Th.	Exp.	Th.	Exp.	Th.	Exp.	Th.	Exp.	Th.
1/2					0.0	0.0		398.5	0.0	0.0	469.8	469.8
3/2					11.4	11.4		454.4	7.9	7.9	492.1	477.7
5/2					56.3	74.6		475.5	57.3	62.8	505.6	498.3
7/2					82.9	106.9		550.3	75.7	108.4	556.0	549.8
9/2	0.0	0.0			162.3	191.2		581.3	163.8	183.5	583.0	572.0
11/2	539.0	545.0			204.1	231.8		680.9	193.5	222.0	661.2	655.2
13/2	234.3	235.0	588.0	586.0	317.3	347.7	721.9	318.5	338.1	698.7	685.7	682.5
15/2	837.0	847.6	495.4	496.0	375.1	393.1	846.4	846.4	359.2	386.5	806.4	799.9
17/2	529.1	525.4	921.0	917.4	518.2	544.2	930.0	899.1	519.5	534.9	857.5	839.5
19/2	1229.0	1210.6	733.7	734.3	592.0	592.0	1027.5	1046.6	570.9	592.2	992.5	984.2
21/2	876.6	861.2	1309.0	1318.9	762.8	780.3	1131.0	1113.3	764.7	773.7	1058.1	1033.3
23/2	1622.0	1626.6	1035.6	1038.3	853.0	829.0	1250.7	1281.3	828.0	839.2	1219.4	1208.3
25/2	1271.6	1235.5	1722.0	1790.5	1048.7	1065.8	1376.1	1364.8	1053.1	1054.4	1300.9	1267.2
27/2	2022.0	2090.7	1393.6	1400.6	1155.1	1108.8	1515.7	1550.2	1127.8	1127.8	1487.4	1472.2
29/2	1684.7	1644.4	2137.0	2230.5	1372.2	1378.3	1662.3	1654.0	1381.5	1377.0	1584.9	1541.2
31/2	2444.0	2600.9	1815.6	1814.2	1494.1	1421.6	1821.8	1852.8	1467.8	1458.0	1795.4	1776.0
33/2	2113.4	2086.8	2552.0	2580.8	1729.2	1728.7	1987.7	1981.0	1748.5	1744.2	1908.9	1855.4
35/2			2272.1	2272.7	1868.2	1772.5	2166.5	2188.9	1847.0	1831.3	2143.4	2119.8
37/2	2563.6	2563.6	2987.0	3115.9	2117.2	2117.2	2349.7	2346.1	2152.2	2150.2	2272.0	2209.8
39/2			2750.8	2770.6	2272.2	2161.7	2547.5	2558.3	2263.0	2245.0	2529.4	2503.6
41/2	3029.0	3076.7			2530.1	2544.1	2746.7	2749.4	2590.1	2597.9	2672.0	2604.4
43/2			3255.8	3303.4	2702.5	2589.4	2960.5	2960.5	2714.0	2700.5	2951.4	2927.5
45/2	3505.0	3627.9			2963.8	3009.5	3174.7	3191.3	3060.1	3087.5	3108.0	3039.3
47/2			3776.5	3867.8	3154.5	3055.6	3401.5	3395.3	3198.0	3198.0	3407.0	3395.3
49/2	4009.6	4218.7			3415.8	3513.7	3630.0	3671.7	3559.1	3619.1	3578.0	3514.4
51/2			4328.9	4462.5	3625.5	3560.5	3865.0	3862.4	3713.0	3737.0	3895.0	3895.8
53/2	4540.4	4759.2			3886.8	4057.8	4105.0	4190.9	4087.1	4194.0	4080.0	4029.9
55/2			4913.6	5044.1	4115.0	4104.8	4344.0	4350.0	4256.0	4319.8	4413.0	4436.7

generated by the intrinsic state $2g_{7/2,1/2}\Psi_g$. Exceptions are the states $33/2^-$ and $37/2^-$, which originate from $1h_{9/2,1/2}\Psi_g$. The results for excitation energies as well as the corresponding experimental data for ^{219}Ra are plotted in Fig. 1.

The case of ^{227}Ra was treated with the formalism presented in Sec. III. The single-particle basis is $2g_{7/2}$, $2g_{9/2}$, and $2f_{5/2}$. The first state coupled to the coherent state describing the unprojected ground state (i.e., $2g_{7/1,1/2}\Psi_g$) generates the parity partner bands $K^\pi = 1/2^\pm$. The bands $K^\pi = 3/2^\pm$ are obtained through projection from the product state $2g_{9/2,-1/2}\Psi_2^{(\gamma;\pm)}$, and the bands $K^\pi = 5/2^\pm$ originate from the intrinsic state $2f_{5/2,1/2}\Psi_2^{(\gamma;\mp)}$. For the bands characterized by $K^\pi = 1/2^\pm$, one could consider also the mixing of components with different K in the manner discussed in Sec. II. However, our numerical application suggests that such a mixing is not really necessary to obtain a realistic description of the available data. The calculated energies in the three bands are compared with the corresponding experimental data in Fig. 2. The plotted values are collected in Table III. The states for ^{227}Ra were obtained in Ref. [4] by using the (n, γ), (d, p), and $(\vec{t}, d)$ reactions and the β^- decay of ^{227}Fr. The spectrum

yielded by these experiments was interpreted in Ref. [8] in terms of a particle-core interaction.

From Fig. 2, we note that our approach reproduces the experimental energies ordering in the band $K^\pi = 1/2^-$. The energy split of the states $3/2^-$ and $1/2^-$ is nicely described, although the doublet is shifted down by about 50 keV. In the band $5/2^+$, an energy level exists that is tentatively assigned as $11/2^+$. Our calculations suggest that this level could be assigned as $13/2^+$. However, this assignment is to be used cautiously because our calculations are not extremely accurate. Moreover, because of the lack of data, there is no one-to-one correspondence between experimental and theoretical levels. No experimental data are available for the band $5/2^-$. In Fig. 2, however, we gave the results of our calculations for this band. Note that the ordering for the lowest levels is not the natural one. However, starting with $13/2^-$, the normal ordering is restored. It is interesting to note that the heading states for the bands $3/2^+$ and $5/2^+$ are almost degenerate. The same is true for the lowest angular momenta states in their negative parity partner bands. The rms deviation for this nucleus is 23 keV.

TABLE III. Excitation energies (keV) in ^{227}Ra for the bands characterized by $K^{\pi} = 1/2^{\pm}$, $3/2^{\pm}$, and $5/2^{\pm}$, respectively. The results of our calculations (Th.) are compared with the corresponding experimental data (Exp.) taken from Ref. [4].

J	K = 1/2				K = 3/2				K = 5/2			
	$\pi = +$		$\pi = -$		$\pi = +$		$\pi = -$		$\pi = +$		$\pi = -$	
	Exp.	Th.	Exp.	Th.	Exp.	Th.	Exp.	Th.	Exp.	Th.	Exp.	Th.
1/2	121	96.6	297	251.8								
3/2	161	145.5	284	232.4	0.0	0.0	90	90				
5/2	177	177.0		359.1	26	26.0	102	102	2	2.		107.6
7/2	268	283.6		310.6	64	40.33		104.6	26.	26.5		86.6
9/2	300	304.6				66.2		115.1	84	61.0		82.8
11/2		574.5				97.9	139	139.1	187	107.5		99.9
13/2						140.5		176.9		160.1		131.1
15/2							228	226.6		221.0		177.5
17/2								288.4		291.4		239.6
19/2										372.3		317.6

Now, we comment on the parameters yielded by the fitting procedure for the considered isotopes. Except for ^{237}U, where both quadrupole-quadrupole and octupole-octupole interactions are attractive, the two interactions have different characters for the rest of the nuclei. In the first situation, the λ $(=2, 3)$-pole moments of the odd nucleon and those of the collective core have different signs. In the remaining cases, the two moments are of the same sign. We also note the large strength for the $q_3 Q_3$ interaction in ^{227}Ra, which is consistent with the fact that the neighboring even-even isotope exhibits a relatively large octupole deformation. Indeed, according to Ref. [20], for this nucleus we have $f = 0.8$. The large value of the strength X_3 determines the large mixing amplitudes of the states $(g_{9/2}\Psi_g^{(+)}; f_{5/2}\Psi_g^{(-)})$ as well as of the states $(g_{9/2}\Psi_g^{(-)}; f_{5/2}\Psi_g^{(+)})$. Indeed, the value obtained for this

amplitude is $|A_{i,3}^{(+)}|^2 = |A_{1,3}^{(-)}|^2 = 0.07425$. Another distinctive feature for ^{227}Ra is that the jJ interaction strength has a sign different from that associated with other nuclei. In fact, the repulsive character of this interaction in ^{227}Ra is necessary to compensate for the large attractive contribution of the $q_3 Q_3$ interaction.

Further, we address the question of whether one could identify signatures for static octupole deformation in the two bands. In Fig. 3, we plot the energy displacement functions [7,16,17]

$$\delta E(I) = E(I^-) - \frac{(I + 1)E[(I - 1)^+] + I E[(I + 1)^+]}{2I + 1},$$
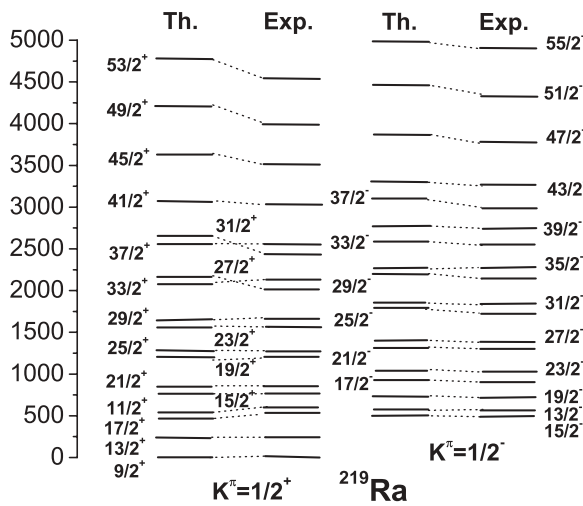
(5.2)

FIG. 1. Calculated (Th.) and experimental (Exp.) excitation energies for the $K^{\pi} = 1/2^{\pm}$ bands in ^{219}Ra. The data were taken from Ref. [2]. The energies of the states $(11/2 + 2k)^+$, $k = 0, 1, 2, \ldots$ and $(13/2 + 2m)^-$, $m = 0, 1, 2, \ldots$ were taken from Ref. [3]. The mentioned states are organized into two bands, I and II, which do not have a definite K. The states shown here belong to band I.
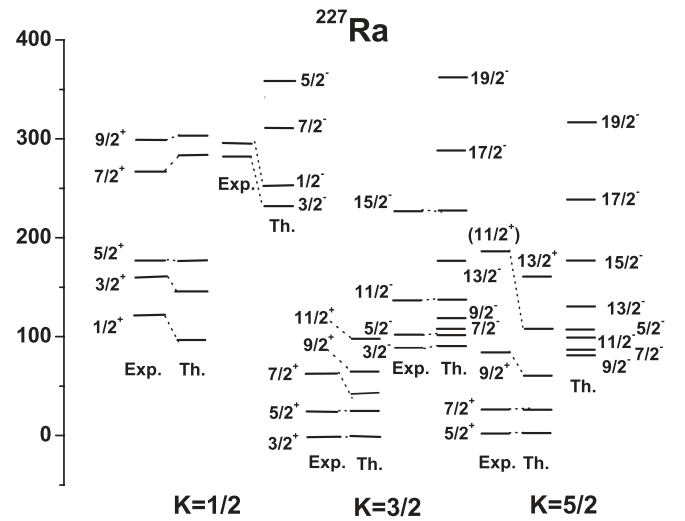

FIG. 2. Calculated (right column) and experimental (left column) excitation energies for the bands with $K^{\pi} = 1/2^{\pm}$, $3/2^{\pm}$, and $5/2^{\pm}$ in ^{227}Ra. The experimental data were taken from Ref. [4]. Data for the $K^{\pi} = 5/2^-$ band are not available, and therefore only the theoretical results are presented. The plot corresponds to the energies listed in Table III.
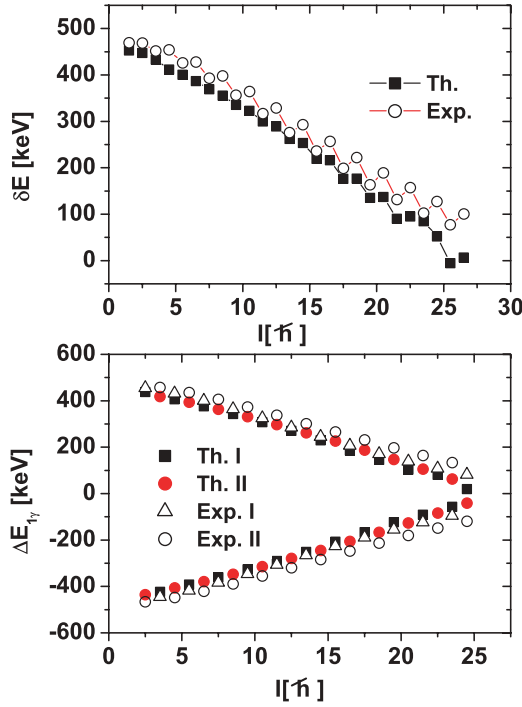
FIG. 3. (Color online) The theoretical and experimental energy displacement functions $\delta E(I)$ and $\Delta E_{1,\gamma}(I)$ given by Eqs. (5.2) and (5.3), respectively, and characterizing the isotope ^{239}Pu plotted as a function of the angular momentum I. Experimental data are taken from Ref. [1]. In the lower panel, the theoretical and experimental $\Delta E_{1,\gamma}(I)$ corresponding to the states $I^\pi = [(1/2) + 2k]^+$ with $k = 1, 2, 3, \ldots$ are represented by the symbols labeled as Th. I and Exp. I, respectively, whereas those associated with the negative parity states $I^\pi = [(1/2) + 2k]^-$ with $k = 1, 2, 3, \ldots$ bear the labels Th. II and Exp. II, respectively.

$$\Delta E_{1,\gamma}(I) = \frac{1}{16}[6E_{1,\gamma}(I) - 4E_{1,\gamma}(I-1) - 4E_{1,\gamma}(I+1)$$
$$+ E_{1,\gamma}(I-2) + E_{1,\gamma}(I+2)], \qquad (5.3)$$
$$E_{1,\gamma}(I) = E(I+1) - E(I).$$

The first function, δE, vanishes when the excitation energies of the parity partner bands depend linearly on $I(I + 1)$ and the moments of inertia of the two bands are equal. Thus, the vanishing value of δE is considered to be a signature for octupole deformation. If the excitation energies depend quadratically on $I(I + 1)$ and the coefficients of the $[I(I + 1)]^2$ terms for the positive and negative parity bands are equal, the second energy displacement function $\Delta E_{1,\gamma}$ vanishes, which again suggests a static octupole deformation. The parities associated with the angular momenta, involved in $\Delta E_{1,\gamma}$ are as follows: Levels I and $I \pm 2$ have the same parity, whereas levels I and $I \pm 1$ are of opposite parity. The results plotted in Fig. 3 correspond to ^{239}Pu. We chose this nucleus because more data are available. The plot suggests that a static octupole deformation is possible for the states with angular momenta $I \geqslant 51/2$ belonging to the two parity partner bands.

Finally, we calculated the branching ratio R_J defined by Eq. (4.1) for ^{219}Ra. There are two parameters involved that

TABLE IV. Experimental (Exp.) and calculated (Present[1] and Present[2]) ratios $B(E1)/B(E2)$ for initial state J^π running from $19/2^-$ up to $51/2^-$. As mentioned in the text, $J_{g.s.} = 9/2$. Experimental data are from Ref. [2]. The results are given in units of 10^{-6} fm^{-2}. For comparison, the results of Ref. [11] are also given in column 4. The theoretical results from columns 2 and 3 correspond to different parameters q_1/q_2 and a characterizing the involved transition operators. These parameters are given in the text.

$J^\pi - J_{g.s.}$	Exp.	Present[1]	Present[2]	Ref. [11]
5^-	2.52(18)	2.52	2.52	1.195
6^+	1.12(08)	1.09	0.677	0.314
7^-	1.49(10)	3.97	3.284	1.318
8^+	1.23(16)	1.23	0.704	0.313
9^-	1.16(08)	4.56	3.194	1.442
10^+	2.77(64)	1.44	0.775	0.312
11^-	1.41(9)	4.59	2.829	1.567
12^+	3.68(26)	1.69	0.868	0.313
13^-	2.14(30)	4.39	2.448	1.691
14^+	1.96(14)	1.96	0.967	0.314
15^-	1.76(18)	4.11	2.131	1.814
16^+	1.06(17)	2.22	1.060	0.315
17^-	2.08(28)	3.84	1.887	1.936
18^+	3.34(48)	2.45	1.137	0.317
19^-	1.34(42)	3.62	1.704	2.057
20^+	2.38(44)	2.63	1.195	0.318
21^-	4.01(94)	3.44	1.568	2.177
Average	2.09(9)	2.97	1.7	1.072

were fixed so that two particular experimental data were reproduced. Thus we fixed alternatively the ratios for the states as $19/2^-$, $37/2^+$ and $19/2^-$, $41/2^+$, respectively. The results corresponding to the two sets of parameters are given in columns 2 and 3 (labeled Present[1] and Present[2]) of Table IV. The values obtained for these parameters are

$$\text{present}^1: \quad \frac{q_1}{q_2} = 18.377 \times 10^{-3} \text{ fm}^{-1},$$
$$ab^2 = -0.63616 \text{ fm}^2,$$
$$\text{present}^2: \quad \frac{q_1}{q_2} = 11.310 \times 10^{-3} \text{ fm}^{-1}, \qquad (5.4)$$
$$ab^2 = -0.34422 \text{ fm}^2,$$

where b denotes the oscillator length characterizing the spherical shell model states for the odd nucleon. As shown in Table IV, the theoretical results agree reasonably well with the corresponding experimental data. Our results show an oscillating behavior with maxima for the negative parity states. Note that some of the data are well described but others deviate from the data by a factor ranging from 2 to 3. In the fourth column of Table IV, we list the results obtained by the authors of Ref. [11] using a different model. In Ref. [11], the ratios corresponding to positive parity states are almost constant and small. The column Present[1] shows a good agreement for the branching of positive parity states, whereas in Ref. [11] better agreement is achieved for negative parity states. This might be because we use different wave functions as well as different transition operators. Another reason might be that we fix the

strengths of the transition operators not by a least squares procedure, which would improve the agreement for negative parity states, but instead by fixing two particular branchings. The branchings are quite sensitive to the choice of the pair of states whose branchings are fitted to the experimental data. We come to this conclusion by comparing the results shown in the columns Present[1] and Present[2] from Table IV. Indeed, the results in Present[2] show better overall agreement than those in Present[1]. Actually, results close to those of Ref. [11] can be obtained by a suitable set of parameters $(q_1/q_2, a)$.

VI. CONCLUSIONS

In the previous sections, we proposed a new formalism for the description of parity partner bands in even-odd nuclei. Our approach uses a particle-core Hamiltonian, with a phenomenological core described in terms of quadrupole and octupole bosons. The single-particle space consists of three spherical shell model states, two of them with positive parity and the third with negative parity. The particle-core coupling terms cause the excitation of the odd particle from one state to either of the remaining two. Thus, the particle-core interaction might break two symmetries for the single-particle motion, the rotation, and space reflection, which is consistent with the structure of the mean field obtained by averaging the model Hamiltonian with quadrupole and octupole boson coherent states. For $K = 1/2$ bands, the single-particle states are coupled to the ground state of a deformed core, whereas for $K = 3/2$ and $5/2$, the single-particle states are coupled to the γ intrinsic state. The bands are generated through angular momentum projection from the particle-core intrinsic states mentioned previously. In this way, the influence of the excited states from the ground band on the structure of $K^\pi = 1/2^\pm$ and that of the excited states from the γ band on the $K^\pi = 3/2^\pm$ and $5/2^\pm$ bands are taken into account. The contribution of various terms of the model Hamiltonian are analyzed in terms of the magnitude and the sign of the interaction strengths yielded by the fitting procedure. Approaches that treat the particle-core interaction in the intrinsic frame of reference stress the role played by the Coriolis interaction, through the decoupling parameter, in determining the energy splitting of the parity partner states with $K = 1/2$. For example, in ^{227}Ra, the decoupling factor is quite high (0.7) [4]. In the laboratory frame, we identified the interaction that determines the energy parity split.

Applications to ^{219}Ra, ^{237}U, and ^{239}Pu show good agreement between the calculated excitation energies in the bands with $K^\pi = 1/2^\pm$ and the corresponding experimental data. The branching ratios of ^{219}Ra have been also calculated. The agreement with the available data is quite good.

For some isotopes, in Ref. [13], only the bands with $K = 5/2$ are considered. In contrast, for ^{227}Ra, we simultaneously treated the bands with $K^\pm = 1/2^\pm, 3/2^\pm,$ and $5/2^\pm$, respectively. Moreover, here the bands with $K = 3/2$ and $5/2$ are generated by coupling a single-particle state to the states belonging to the γ band of the core system.

The plot for the energy displacement functions, or energy staggering factors, made for ^{239}Pu indicates that a static

octupole deformation might be set for states with angular momentum greater than $51/2\hbar$.

Before closing, we add few remarks about the possible development of the present formalism. By choosing the generating states for the parity partner bands with $K^\pi = 0^\pm_\beta, 1^\pm$ states for the core unprojected states, and otherwise keeping the same single-particle basis for the odd nucleon, the present formalism can be extended to another four bands, two of positive parity and two of negative parity. Another noteworthy remark refers to the chiral symmetry [24] for the composite particle and core system. Indeed, in Ref. [20] we showed that, starting from a certain total angular momentum of the core, the angular momenta carried by the quadrupole ($\vec{J}_2$) and octupole ($\vec{J}_3$) bosons are perpendicular to each other. Naturally, we may ask ourselves whether there exists a strength for the particle-core interaction such that the angular momentum of the odd particle becomes perpendicular to the plane ($\vec{J}_2, \vec{J}_3$). This would be a sign that the three-component system exhibits chiral symmetry.

One may say that the present CSM extension to odd nuclei can describe quite well the excitation energies in the parity partner bands with $K^\pi = 1/2^\pm, 3/2^\pm,$ and $5/2^\pm$.

APPENDIX A

The diagonal matrix elements of the quadrupole-quadrupole ($q_2 Q_2$) and octupole-octupole ($q_3 Q_3$) particle-core interactions in the basis defined in Sec. III are

$$
\begin{aligned}
&\langle \varphi^{(\pm)}_{IM; j_i K} | q_2 Q_2 | \varphi^{(\pm)}_{IM; j_i K} \rangle \\
&= -X_2 C^{j_i \, J \, I}_{k-2 \, 2 \, K} C^{j_i \, J' \, I}_{k-2 \, 2 \, K} \hat{I}^2 \hat{j}_i \hat{J} W(j_i I 2 J; J' j_i) \\
&\quad \times (N^{(\pm)}_{I,K})^2 \left(N^{(\gamma,\pm)}_J N^{(\gamma,\pm)}_{J'}\right)^{-1} \\
&\quad \times \langle j_i || r^2 Y_2 || j_i \rangle \langle \varphi^{(\gamma;\pm)}_J || b_2^\dagger + b_2 || \varphi^{(\gamma;\pm)}_{J'} \rangle, \\
&\qquad i = 2, 3, \quad K = i - 1/2; \quad\quad\quad (A1)
\end{aligned}
$$

$$
\begin{aligned}
&\langle \varphi^{(\pm)}_{IM; j_3 5/2} | q_3 Q_3 | \varphi^{(\pm)}_{IM; j_2 3/2} \rangle \\
&= X_3 C^{j_3 \, J \, I}_{1/2 \, 2 \, 5/2} C^{j_2 \, J' \, I}_{-1/2 \, 2 \, 3/2} \hat{I}^2 \hat{j}_3 \hat{J} W(j_2 I 3 J; J' j_3) \\
&\quad \times N^{(\pm)}_{I,5/2} N^{(\pm)}_{I,3/2} \left(N^{(\gamma,\pm)}_J N^{(\gamma,\pm)}_{J'}\right)^{-1} \langle j_3 || r^3 Y_3 || j_i \rangle \\
&\quad \times \langle \varphi^{(\gamma;\pm)}_J || b_3^\dagger + b_3 || \varphi^{(\gamma;\mp)}_{J'} \rangle.
\end{aligned}
$$

The expected value for the $q_2 Q_2$ term in the state $\varphi^\pm_{IM; j_1 1/2}$ can be obtained from this expression by replacing j_i with j_1 and $\varphi^{(\gamma;\pm)}_J$ with $\varphi^{(g;\pm)}_J$. Also, the projections associated with J and J' in the two Clebsch-Gordan coefficients should be equal to 0, not 2. It is easy to check that this state is not connected by the $q_3 Q_3$ interaction to the state $\varphi^\pm_{IM; j_3 5/2}$. The reduced matrix elements of the boson operators involved in these equations

have the expressions

$$
\langle \varphi_J^{(\gamma;\pm)} || b_2^\dagger + b_2 || \varphi^{(\gamma;\pm)} \rangle
$$

$$
= d C_{2\,0\,2}^{J'\,2\,J} \left\{ \frac{N_J^{(\gamma;\pm)}}{N_{J'}^{(\gamma;\pm)}} + \frac{2J'+1}{2J+1} \frac{N_{J'}^{(\gamma;\pm)}}{N_J^{(\gamma;\pm)}} \right.
$$

$$
+ \frac{6}{7} \sum_{J'} \frac{N_J^{(\gamma;\pm)} N_{J'}^{(\gamma;\pm)}}{N_{J_1}^{(g;\pm)}}
$$

$$
\left. \times \left[(C_{0\,2\,2}^{J_1\,2\,J'})^2 + \frac{2J'+1}{2J+1} (C_{0\,2\,2}^{J_1\,2\,J'})^2 \right] \right\},
$$

$$
\langle \varphi_J^{(g;\pm)} || b_2^\dagger + b_2 || \varphi_{J'}^{(g;\pm)} \rangle
$$

$$
= d C_{0\,0\,0}^{J'\,2\,J} \left[\frac{N_J^{(g;\pm)}}{N_{J'}^{(g;\pm)}} + \frac{2J'+1}{2J+1} \frac{N_{J'}^{(g;\pm)}}{N_J^{(g;\pm)}} \right],
$$

$$
\langle \varphi_J^{(\gamma;+)} || b_3^\dagger + b_3 || \varphi_{J'}^{(\gamma;-)} \rangle \qquad \text{(A2)}
$$

$$
= f C_{2\,0\,2}^{J'\,2\,J} \left[\frac{N_J^{(\gamma;+)}}{N_{J'}^{(\gamma;-)}} + \frac{2J'+1}{2J+1} \frac{N_{J'}^{(\gamma;-)}}{N_J^{(\gamma;+)}} \right],
$$

$$
\langle \varphi_J^{(\gamma;-)} || b_3^\dagger + b_3 || \varphi_{J'}^{(\gamma;+)} \rangle
$$

$$
= (-)^{J'-J} \frac{\hat{J'}}{\hat{J}} \langle \varphi_{J'}^{(\gamma;+)} || b_3^\dagger + b_3 || \varphi^{(\gamma;-)} \rangle,
$$

$$
\langle \varphi_J^{(g;+)} || b_3^\dagger + b_3 || \varphi_{J'}^{(g;-)} \rangle
$$

$$
= f C_{0\,0\,0}^{J'\,2\,J} \left[\frac{N_J^{(g;+)}}{N_{J'}^{(g;-)}} + \frac{2J'+1}{2J+1} \frac{N_{J'}^{(g;-)}}{N_J^{(g;+)}} \right],
$$

$$
\langle \varphi_J^{(g;-)} || b_3^\dagger + b_3 || \varphi_{J'}^{(g;+)} \rangle
$$

$$
= (-)^{J'-J} \frac{\hat{J'}}{\hat{j}} \langle \varphi_{J'}^{(g;+)} || b_3^\dagger + b_3 || \varphi_J^{(g;-)} \rangle.
$$

The matrix elements of H_{core} have the expressions

$$
\langle \varphi_{IM,j_2 3/2}^{(\pm)} | H_{\text{core}} | \varphi_{IM,j_2 3/2}^{(\pm)} \rangle = N_{I;j_2 3/2}^{(\pm)} \sum_J (C_{-1/2\,2\,3/2}^{j_2\,J\,I})^2
$$

$$
\times \left[N_J^{(\gamma;\pm)} \right]^{-2} E_J^{(\gamma,\pm)},
$$

$$
\langle \varphi_{IM,j_3 5/2}^{(\pm)} | H_{\text{core}} | \varphi_{IM,j_3 5/2}^{(\pm)} \rangle = N_{I;j_3 5/2}^{(\pm)} \sum_J (C_{1/2\,2\,5/2}^{j_2\,J\,I})^2
$$

$$
\times \left[N_J^{(\gamma;\pm)} \right]^{-2} E_J^{(\gamma,\pm)},
$$

$$
\langle \varphi_{IM,j_1 1/2}^{(\pm)} | H_{\text{core}} | \varphi_{IM,j_1 1/2}^{(\pm)} \rangle = N_{I;j_1 1/2}^{(\pm)} \sum_J (C_{1/2\,0\,1/2}^{j_2\,J\,I})^2
$$

$$
\times \left[N_J^{(g;\pm)} \right]^{-2} E_J^{(g,\pm)}, \qquad \text{(A3)}
$$

where $E_J^{(g,\pm)}$ and $E_J^{(\gamma,\pm)}$ denote the energies of the state $J^\pm$ belonging to the bands $g^\pm$ and $\gamma^\pm$, respectively. Obviously, the term H_{sp} is diagonal in the chosen basis:

$$
\langle \varphi_{IM,j_1 1/2}^{(\pm)} | H_{\text{sp}} | \varphi_{IM,j_1 1/2}^{(\pm)} \rangle = \epsilon_{j_1},
$$

$$
\langle \varphi_{IM,j_2 3/2}^{(\pm)} | H_{\text{sp}} | \varphi_{IM,j_2 3/2}^{(\pm)} \rangle = \epsilon_{j_2}, \qquad \text{(A4)}
$$

$$
\langle \varphi_{IM,j_3 5/2}^{(\pm)} | H_{\text{sp}} | \varphi_{IM,j_3 5/2}^{(\pm)} \rangle = \epsilon_{j_3}.
$$

Here ϵ_{j_k} denotes the energies of the spherical shell model states $|n_k, l_k, j_{k}, m_{k}\rangle$ with $k = 1, 2,$ and 3. The matrix elements of the term $\vec{j} \cdot \vec{J}$ are

$$
\langle \varphi_{IM,j_1 1/2}^{(\pm)} | \vec{j} \cdot \vec{J} | \varphi_{IM,j_1 1/2}^{(\pm)} \rangle = \frac{1}{2} \left\{ I(I+1) - j_1(j_1+1) \right.
$$

$$
- N_{I;j_1 1/2}^{(\pm)} \sum_J (C_{1/2\,0\,1/2}^{j_2\,J\,I})^2
$$

$$
\left. \times \left[N_J^{(g;\pm)} \right]^{-2} J(J+1) \right\},
$$

$$
\langle \varphi_{IM,j_2 3/2}^{(\pm)} | \vec{j} \cdot \vec{J} | \varphi_{IM,j_2 3/2}^{(\pm)} \rangle = \frac{1}{2} \left\{ I(I+1) - j_2(j_2+1) \right.
$$

$$
- N_{I;j_2 3/2}^{(\pm)} \sum_J (C_{-1/2\,2\,3/2}^{j_2\,J\,I})^2
$$

$$
\left. \times \left[(N_J^{(\gamma;\pm)})^{-2} J(J+1) \right] \right\},
$$

$$
\langle \varphi_{IM,j_3 5/2}^{(\pm)} | \vec{j} \cdot \vec{J} | \varphi_{IM,j_3 5/2}^{(\pm)} \rangle = \frac{1}{2} \left\{ I(I+1) - j_3(j_3+1) \right.
$$

$$
- N_{I;j_3 5/2}^{(\pm)} \sum_J (C_{1/2\,2\,5/2}^{j_2\,J\,I})^2
$$

$$
\left. \times \left[N_J^{(\gamma;\pm)} \right]^{-2} J(J+1) q \right\}.
$$

$$
\text{(A5)}
$$

APPENDIX B

The matrix elements involved in the expression of the branching ratios are

$$
\langle \varphi_I^{(\pi)}(j_i K; d, f) || r^2 Y_2 || \varphi_{I'}^{(\pi)}(j_i K'; d, f) \rangle
$$

$$
= -\sqrt{\frac{5}{4\pi}} \langle r^2 \rangle \hat{I'} \hat{j}_i N_{i,IK}^{(\pi)} N_{i,I'K'}^{(\pi)}
$$

$$
\times \sum_J C_{K\,0\,K}^{j_i\,J\,I} C_{K'\,0\,K'}^{j_i\,J\,I'} \left[N_J^{(g,\sigma)} \right]^{-2},
$$

$$
\langle \varphi_I^{(\pi)}(j_i K; d, f) || b_2^\dagger + b_2 || \varphi_{I'}^{(\pi)}(j_i K'; d, f) \rangle \qquad \text{(B1)}
$$

$$
= d C_{K\,0\,K}^{I'\,2\,I} \left[\frac{N_{i;IK}^{(\pi)}}{N_{i;I'K'}^{(\pi)}} + \frac{2I'+1}{2I+1} \frac{N_{i;I'K'}^{(\pi)}}{N_{i;IK}^{(\pi)}} \right],
$$

$$
\langle \varphi_I^{(\pi)}(j_i K; d, f) || (b_2^\dagger b_3^\dagger)_1 + (b_3 b_2)_1 || \varphi_{I'}^{(\pi')}(j_i K'; d, f) \rangle
$$

$$
= d f C_{K\,0\,K}^{I'\,1\,I} C_{0\,0\,0}^{2\,3\,1} \left[\frac{N_{i;IK}^{(\pi)}}{N_{i;I'K'}^{(\pi')}} + \frac{2I'+1}{2I+1} \frac{N_{i;I'K'}^{(\pi')}}{N_{i;IK}^{(\pi)}} \right].
$$

[1] S. Zhu *et al.*, Phys. Lett. **B618**, 51 (2005).

[2] P. D. Cottle *et al.*, Phys. Rev. C **36**, 2286 (1987).

[3] M. Wieland *et al.*, Phys. Rev. C **45**, 1035 (1992).

[4] T. von Egidy *et al.*, Nucl. Phys. **A365**, 26 (1981).

[5] A. A. Raduta, V. Ceausescu, and R. M. Dreizler, Nucl. Phys. **A272**, 11 (1976).

[6] G. A. Leander *et al.*, Nucl. Phys. **A388**, 452 (1982).

[7] D. Bonatsos, C. Daskaloyannis, S. B. Drenska, N. Karoussos, N. Minkov, P. P. Raychev, and R. P. Roussev, Phys. Rev. C **62**, 024301 (2000).

[8] G. A. Leander and Y. S. Chen, Phys. Rev. C **37**, 2744 (1988).

[9] S. Cwiok and W. Nazarewicz, Nucl. Phys. **A529**, 95 (1991).

[10] A. Ya. Dzyublik and V. Yu. Denisov, Yad. Fiz. **56**, 30 (1993) [Phys. At. Nucl. **56**, 303 (1993)].

[11] V. Yu. Denisov and A. Ya. Dzyublik, Yad. Fiz. **56**, 96 (1993) [Phys. At. Nucl. **56**, 477 (1993)].

[12] V. Yu. Denisov and A. Ya. Dzyublik, Nucl. Phys. **A589**, 17 (1995).

[13] N. Minkov, S. Drenska, P. Yotov, S. Lalkovski, D. Bonatsos, and W. Scheid, Phys. Rev. C **76**, 034324 (2007).

[14] A. A. Raduta, V. Ceausescu, A. Gheorghe, and R. M. Dreizler, Phys. Lett. **B99**, 444 (1981); Nucl. Phys. **A381**, 253 (1982).

[15] A. A. Raduta, A. H. Raduta, and A. Faessler, Phys. Rev. C **55**, 1747 (1997).

[16] A. A. Raduta, D. Ionescu, and A. Faessler, Phys. Rev. C **65**, 064322 (2002).

[17] A. A. Raduta and D. Ionescu, Phys. Rev. C **67**, 044312 (2003).

[18] A. A. Raduta, D. Ionescu, I. I. Ursu, and A. Faessler, Nucl. Phys. **A720**, 43 (2003).

[19] A. A. Raduta and C. M. Raduta, Nucl. Phys. **A768**, 170 (2006).

[20] A. A. Raduta, A. H. Raduta, and C. M. Raduta, Phys. Rev. C **74**, 044312 (2006).

[21] A. A. Raduta, A. R. Raduta, and A. H. Raduta, Phys. Rev. B **59**, 8209 (1999).

[22] M. E. Rose, *Elementary Theory of Angular Momentum* (John Wiley & Sons, Inc., New York, 1957).

[23] P. Ring and P. Schuck, *The Nuclear Many-Body Problem* (Springer, Berlin, 2000), p. 76.

[24] S. Frauendorf and J. Meng, Nucl. Phys. **A617**, 131 (1997).